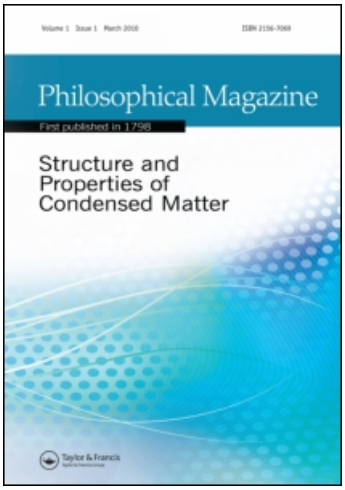

Philosophical Magazine
Publication details, including instructions for authors and subscription information:
http://www.informaworld.com/smpp/title~content=t713695589

Ab initio pseudopotential study of vacancies and self-interstitials in hcp titanium

Abdulrafiu Tunde Raji[a]; Sandro Scandolo[b]; Riccardo Mazzarello[c]; Schadrack Nsengiyumva[a]; Margit Härting[a]; David Thomas Britton[a]
[a] Department of Physics, University of Cape Town, Cape Town, South Africa [b] Condensed Matter and Statistical Physics Section (CMSP), The Abdus Salam International Centre for Theoretical Physics (ICTP), Strada Costiera 11, 34014 Trieste, Italy [c] International School for Advanced Studies (SISSA), Via Beirut 4, 34014 Trieste, Italy

To cite this Article Tunde Raji, Abdulrafiu , Scandolo, Sandro , Mazzarello, Riccardo , Nsengiyumva, Schadrack , Härting, Margit and Thomas Britton, David(2009) '*Ab initio* pseudopotential study of vacancies and self-interstitials in hcp titanium', Philosophical Magazine, 89: 20, 1629 — 1645
To link to this Article: DOI: 10.1080/14786430903019032
URL: http://dx.doi.org/10.1080/14786430903019032

Philosophical Magazine
Vol. 89, No. 20, 11 July 2009, 1629–1645

Taylor & Francis
Taylor & Francis Group

Ab initio pseudopotential study of vacancies and self-interstitials in hcp titanium

Abdulrafiu Tunde Raji[a]*, Sandro Scandolo[b], Riccardo Mazzarello[c]†, Schadrack Nsengiyumva[a], Margit Härting[a] and David Thomas Britton[a]

[a]*Department of Physics, University of Cape Town, Private Bag X3, Rondebosch 7701, Cape Town, South Africa;* [b]*Condensed Matter and Statistical Physics Section (CMSP), The Abdus Salam International Centre for Theoretical Physics (ICTP), Strada Costiera 11, 34014 Trieste, Italy;* [c]*International School for Advanced Studies (SISSA), Via Beirut 4, 34014 Trieste, Italy*

(*Received 19 February 2008; final version received 5 May 2009*)

By means of an *ab initio* plane-wave pseudopotential method, monovacancy, divacancy and self-interstitials in hcp titanium are investigated. The calculated monovacancy formation energy is 1.97 eV, which is in excellent agreement with other theoretical calculations, and agrees qualitatively with published experimental results. The relaxation of the atoms around a single vacancy is observed to be small. Two divacancy configurations, the in-plane and the off-plane, have also been shown to be equally stable. With regards to the interstitials, of the eight configurations studied, two (octahedral and basal octahedral) have relatively lower formation energies and are, thus, the most likely stable configurations. We find small energy differences between them, suggesting their possible co-existence. It is also observed that the tetrahedral configuration decays to a split dumbbell configuration, whereas both the basal tetrahedral and the basal pseudocrowdion interstitials decay to the basal octahedral configuration. Using the nudged elastic band method (NEB), we determine a possible minimum energy path (MEP) for the diffusion of self-interstitial titanium atoms from an octahedral site to the nearest octahedral site. The energy barrier for this migration mechanism is shown to be about 0.20 eV.

Keywords: self-interstitial; *ab initio*; density-functional theory; ion implantation; point defects; residual stress; titanium

1. Introduction

Advances in computational techniques and resources have enabled detailed first principles studies of important defect properties in both simple and transition metals [1]. These defects may include vacancies, interstitials, dislocations and grain boundaries. These advances could help in closing the gap between macroscopic and microscopic theories seeking to elaborate, and link, the different length scales

*Corresponding author. Email: abdulrafiu.raji@uct.ac.za
†Present address: Computational Science, Department of Chemistry and Applied Biosciences, ETH Zurich, USI Campus, Via Giuseppe Buffi 13, CH-6900 Lugano, Switzerland.

ISSN 1478–6435 print/ISSN 1478–6443 online

DOI: 10.1080/14786430903019032
http://www.informaworld.com

determining material properties. For instance, we can use basic ground state and defect properties of materials, calculated from first principles electronic structure techniques, to develop quantum-based interatomic potentials that can be applied in molecular dynamics studies [2] of extended defects, and defect–defect interactions, involving thousands of atoms [3]. These results, in turn, can provide fundamental input into mesoscale and macroscale simulations of mechanical properties for the material under consideration.

The properties of perfect crystals can be obtained from standard first principles density functional theory (DFT) calculations. However, calculations for point defects are much more difficult due to the loss of translational symmetry. The problem is usually solved by using either the supercell [4,5] or Green's functions methods [6]. The knowledge of the properties of vacancies and interstitials is necessary for understanding the thermodynamic and kinetic behaviour of metals and alloys [7,8]. These properties include their structure and mobility, as well as the interactions they can have with other defects or foreign atoms. A particularly important property is the formation energy, which determines the specific equilibrium defect concentration. The vacancy formation energy also contributes to the self-diffusion coefficient for the monovacancy mechanism [9], which is the main diffusion process in closed packed metals. However, it is not easy to determine, experimentally with precision, atomic quantities such as the formation energy of a single vacancy or that of an interstitial. This is because these quantities are affected by the local environment, such as the presence of impurities around the defect. Very pure samples are therefore required to obtain reliable results [5].

Under normal conditions, self-interstitials are relatively rare in metals compared to vacancies [10]. However, large densities of both vacancies and self-interstitial atoms (SIAs) are produced in materials subjected to ion implantation [11], or high energy radiation environments [12]. In the latter, it has been observed [10] that SIAs are faster, which means that they have migration energy lower than that of vacancies. Ion implantation is a low temperature, non-equilibrium process, by which almost any element can be introduced into the near surface region of a material. Depending on the implantation dose, the displacement of host atoms can lead to the formation of vacancies and interstitials [13], whose long time evolution into voids and clusters affects the mechanical properties of the implanted materials, such as inducing a change in the local strain. The internal stress state of the material is, thus, modified.

We have recently started a programme to investigate the change in residual stress due to implanted krypton ions in hcp titanium [14] and also to study the different equilibrium point defect configurations resulting from the implantation. In this framework, as a first step, we aim to gain insights into the various defect configurations which may exist in hcp titanium. We have, thus, focused on the calculations of mono and divacancy, as well as the self-interstitial formation energies in hexagonal closed packed titanium, using first principles techniques and the supercell approach. We also calculate the formation volumes, as well as the structural relaxation around the defects. Using the nudged elastic band method (NEB) [15], the minimum energy path (MEP) for one of the possible mechanisms involved in self-interstitial diffusion was also determined.

Relative to cubic metals, there have been far fewer studies on point defects in hexagonal closed packed materials, and among the hexagonal closed packed

materials, zirconium has attracted the most attention owing to its importance in the nuclear industry [12]. An earlier but related study by Tome [16] includes vacancy and interstitial configurations in hcp metals using empirical potentials. More recent investigations include studies on point defect diffusion in α-Ti by Fernandez [17], using the embedded atom method. Similar studies include *ab initio* pseudopotential studies on hcp zirconium by Domain et al. [12] and Willaime [18]. To the authors' knowledge, the present work is the first *ab initio* pseudopotential study of vacancy, divacancy and self-interstitial configurations in hcp titanium.

In this paper, after describing the computational procedures used, results for defect free α-Ti are presented as a test of the calculations. These include calculations of the lattice parameters and elastic constants, which are compared with previous *ab initio* calculations and published experimental data**.** Results concerning mono and divacancy formation energies and volumes, binding energies, self-interstitial formation energies and volumes, as well as self-interstitial atom migration, are then presented and discussed. In this study, convergences of the defect formation energies with respect to the cell sizes were also confirmed.

2. Methods

Eight different self-interstitial and three divacancy configurations were considered. They are shown in Figures 1 and 2, respectively. In naming the self-interstitials, we have adopted the notation of Johnson and Beeler [19]. The self-interstitial site marked as O has an octahedral coordination; the interstitial site S denotes a $\langle 001 \rangle$ split dumbbell, and has two atoms sharing the same site in the *c* direction; C is often termed as pseudocrowdion, and is the site midway between the two nearest neighbour atoms out of the basal plane; while T has a tetrahedral coordination. BT, BC and BO are basal projections of tetrahedral, pseudocrowdion and octahedral configurations, respectively. BS is the split dumbbell, which involves two atoms equidistant from a vacant site, aligned in perpendicular direction to the *c*-axis. The three divacancy configurations are termed the in-plane, the off-plane and the basal–basal. They are denoted as D_{v1}, D_{v2} and D_{v3}, respectively. In the in-plane configuration (D_{v1}), two nearest adjacent atoms of the same plane are missing; the off-plane configuration (D_{v2}) has one atom missing at the basal plane, and the other atom at the nearest off basal plane. In the basal–basal (D_{v3}) configuration, there are two missing atoms at the centre of two basal planes at distance *c,* where *c* is the lattice parameter of the hcp structure. D_{v2}, D_{v1} and D_{v3} thus correspond to divacancy at first, second and fourth nearest neighbours, respectively**.**

All the DFT calculations were performed with the QUANTUM-ESPRESSO package [20]. We used an ultrasoft pseudopotential (PP) of the Vanderbilt type [21] that considers $4s^2$, $3d^2$, and the semi-core states ($3s^2$ and $3p^6$), in the valence band. The PP method is implemented in a plane-wave basis set. We used the exchange-correlation functional, developed by Perdew and Wang [22], in the framework of the generalised gradient approximation (GGA). Regarding the cutoff energy for the plane-wave basis set, we performed extensive convergence studies with values up to 612 eV, but convergence with respect to the total energy, within 2 meV per atom, was achieved for 476 eV. Hence, this value is used throughout the work presented here. In addition,

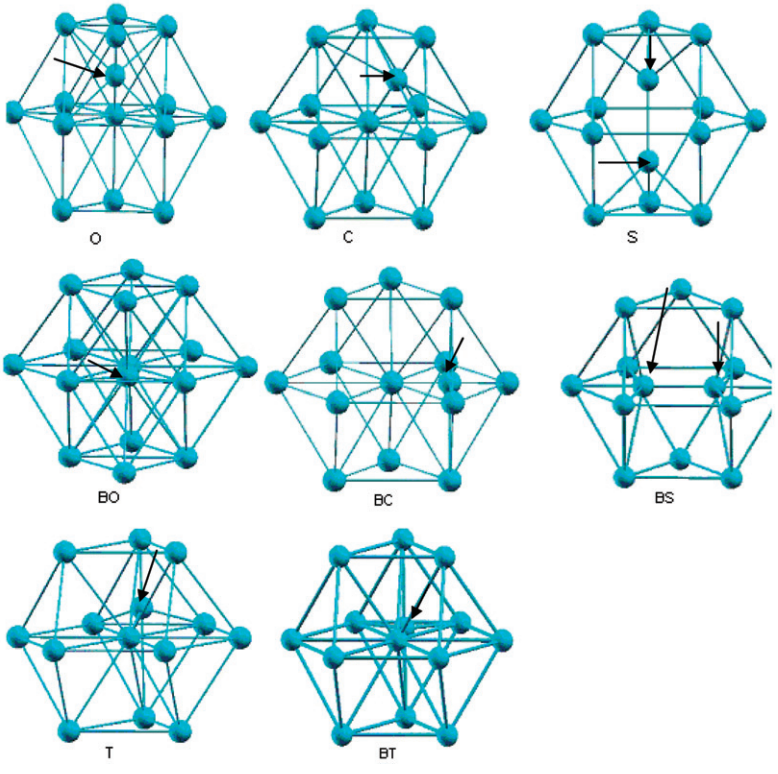

Figure 1. Schematics of the initial eight interstitial configurations in the hcp structure investigated in this study. The interstitials are indicated by the arrows.

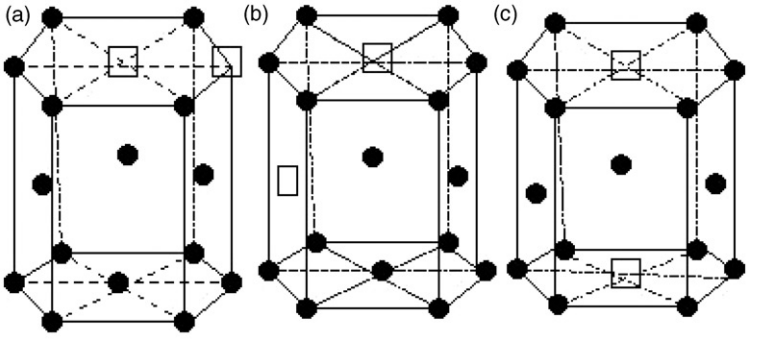

Figure 2. Divacancy configurations (a) D_{v1}, (b) D_{v2} and (c) D_{v3} in the hexagonal closed packed structure, as studied in this work. Filled black circles (•) are regular atomic sites, while open squares (□) are vacancy positions.

convergence of the total energy (within 2 meV) per atom with respect to the discrete Brillouin zone (BZ) sampling was achieved with an $8 \times 8 \times 8$ Monkhorst–Pack [23] grid. This corresponds to 80 irreducible k-points. Equivalent k-points meshes were used for the supercells employed to study various defects configurations.

We have allowed full relaxation of the atomic positions around the defects, as well as the relaxation of the lattice parameters. This was performed by varying the cell lattice parameters, while allowing atomic relaxations and determining the total energy. The minimum of the energy–volume parabolic curve was then chosen as the relaxed configuration of the supercell with a defect. For a given structure, the positions of the atoms were determined by minimising the forces on the ions, using the conjugate gradient algorithm as implemented in the QUANTUM-ESPRESSO code. The structural parameters were considered to be fully relaxed when the forces on the ions were less than 0.05 eV/Å, and the total pressure in the system was less than 1 kbar. During the relaxation runs, the Brillouin zone (BZ) integration was done using the Methfessel–Paxton scheme [24], with a smearing of 0.26 eV.

The Climbing Image Nudged Elastic Band (CI-NEB) [25] method was used to describe the minimum energy paths (MEPs) and the transition states for migration of self-interstitial titanium atoms between two stable configurations. The NEB method is a reliable method of finding the MEP, when the initial and final states of a process are known. An interpolated chain of configurations, commonly referred to as images, between the initial and final positions is connected by springs and relaxed simultaneously to the minimum energy path. With the climbing image scheme, the highest-energy image climbs uphill to the saddle point. In this study, five images were used to determine the MEP, and the migration barrier energy of diffusing self-interstitial titanium atoms. We have used a supercell containing 64 atomic sites and a $2 \times 2 \times 2$ k points mesh. All the images are relaxed until the maximum force acting on an atom is less than 0.05 eV/Å.

The five independent elastic constants of the hcp structure are calculated with the strain matrices proposed by Fast et al. [26]. Deformations preserving the hexagonal symmetry of the cell were used to calculate $C_{11} + C_{12}$, C_{33} and B, while triclinic and monoclinic deformations are used, respectively, for C_{44} and C_{11}–C_{12}. Since α-phase Ti is not centrosymmetric, internal relaxations were allowed for each deformation of the cell. The elastic constants were obtained from a third order polynomial fit, performed over the energies calculated for nine values of the strain ranging from -2% to $+2\%$. The equilibrium lattice parameter and the bulk modulus were obtained from the calculation of the total energy as a function of volume. These results are then fitted to the Murnaghan's [27] equation, which in turn gives the equilibrium atomic volume (Ω_0), the equilibrium energy, the bulk modulus (B_0) and its derivative with respect to pressure (B_0'). For an hcp structure, there is an additional parameter to be optimised at any given volume, the c/a ratio, where a is the distance between the two nearest atoms in the same basal plane. The energy as a function of the c/a ratio was fitted to the polynomial of the form,

$$E(c/a) = \alpha(c/a)^3 + \beta(c/a)^2 + \gamma(c/a) + \lambda, \tag{1}$$

where α, β, γ and λ are fitting parameters. The c/a ratio corresponding to the minimum energy is the equilibrium ratio for titanium at that volume. If we define N as the total number of atoms in a perfect supercell, the vacancy formation enthalpy can be calculated by using the expression [28],

$$H_{nv}^{f} = E(N-n, n, V') - \frac{N-n}{N} E(N, 0, N\Omega_0) + p(V' - (N-n)\Omega_0), \tag{2}$$

where $E(N-n, n, V')$ denotes the total energy of a relaxed supercell, obtained by removing n atoms from an ideal supercell initially consisting of N atoms. The volume V' corresponds to the equilibrium volume of the supercell at pressure p; Ω_0 is the equilibrium volume of one atom at pressure p in the perfect lattice; $n=1$, 2 for the mono and divacancy, respectively. For the interstitial configurations, the formation energy is defined as

$$H^f_{nv} = E(N+n, n, V') - \frac{N+n}{N} E(N, 0, N\Omega_0) + p(V' - (N+n)\Omega_0). \tag{3}$$

Here, $E(N+n, n, V')$ denotes the total energy of a relaxed supercell, obtained by adding n atoms. In this work, all calculations are performed at zero pressure and, thus, $H^f_{1v} = E^f_{1v}$ is the vacancy formation energy, and $H^f_{2v} = E^f_{2v}$ is the divacancy formation energy.

The vacancy or interstitial formation volume can be defined via the change in the macroscopic dimensions upon its formation, where, for a precise definition, the geometry of the sample must be specified. For supercell geometry, it is defined as

$$\Omega^f_{nv} = V' - (N-n)\Omega_0, \tag{4}$$

for vacancy defects, with $n=1$, 2 for the mono and divacancy, respectively. For interstitial defects, the formation volume is defined as

$$\Omega^f_{ni} = V' - (N+n)\Omega_0, \tag{5}$$

where n is the number of extra atoms inserted into the supercell. The relaxation (contraction) volume due to a defect formation is expressed as $\Omega_0 - \Omega^f_{nv}$ for a monovacancy and $\Omega_0 + \Omega^f_{ni}$ for an interstitial. Attraction between defects is quantified through calculations of binding energies, E^B_{2v}, which are defined as follows:

$$E^B_{2v} = 2E^f_{1v} - E^f_{2v}, \tag{6}$$

where E^f_{1v} and E^f_{2v} are mono and divacancy formation energies, respectively. According to this definition, a positive or negative binding energy implies a stable or metastable divacancy configuration with respect to two isolated monovacancies, respectively.

In any defect-related calculations, the size of the supercell N should be large enough to minimise the interactions between the defects. Supercells consisting of up to $N=96$ atomic sites were used to study the monovacancy properties and convergence with respect to cell size, while supercell of size $N=64$ atomic sites have been used in studying D_{v1} and D_{v2} divacancies, and $N=72$ was used for the D_{v3} configuration. For the interstitials, cells of sizes $N=36$, 64 and 96 were used. The smallest supercell consists of 16 Ti atoms, and has dimensions $2a \times a\sqrt{3} \times 2c$, where a and c represent the calculated lattice parameters. The second supercell, $N=36$ has dimensions $3a \times 3a \times 2c$, while the supercell with 48 atoms measures $3a \times 2a\sqrt{3} \times 2c$. Supercells of sizes $N=64$, 72 atoms have dimensions $4a \times 2a\sqrt{3} \times 2c$, $3a \times 2a\sqrt{3} \times 3c$, respectively. The dimensions of $N=96$ supercells used for the monovacancy and the interstitial are, respectively, $3a \times 2a\sqrt{3} \times 4c$ and $4a \times 2a\sqrt{3} \times 2c$. We have calculated the formation energies for a monovacancy and

three different divacancy configurations denoted as D_{v1}, D_{v2} and D_{v3} (shown in Figure 2). The binding energies of the three divacancy configurations were also determined, while the formation energies and relaxation volumes of eight different interstitial configurations were also calculated. The formation energy predicts the thermodynamically preferred defect structure in a material [29], while the binding energy gives an indication of the stability of a particular defect configuration with respects to its constituents [30]. Convergences of defect formation energies with respect to the cell sizes were confirmed.

3. Structural parameters

The lattice parameters and relative phase stabilities of α-phase titanium were evaluated, the results being displayed in Table 1. The curves of $E(a)$ at $c/a = 1.587$ Å and $E(c/a)$ at $a = 2.950$ Å, from which the lattice parameters are deduced, are also shown in Figure 3. Agreements with experiment [31] are generally good (within an error of ~2%). These results are also in good agreement with previous *ab initio* calculations performed using the linearised augmented-plane-wave (LAPW) [32] and the GGA full-potential-linear-muffin-tin (FP-LMTO) methods [33,34]. FP-LMTO is generally considered more accurate than pseudopotential-based methods. Our GGA calculation, however, predicts a stable ω phase, under zero external pressure, in contrast to experimental results [35]. The energy difference between the α and ω phases is, however, very small (~0.01 eV). Also, from the available experimental data [36], the ω phase is higher in energy than the α phase by ~0.02 eV/atom. Thus, the error we make in the calculation is approximately 0.03 eV/atom; this is still within the accuracy of our DFT calculations. In addition, *ab initio* pseudopotential calculation of Trinkle et al. [37] shows the ω phase to be slightly lower in energy than the α phase at zero external pressure. It should be mentioned also that GGA corrections usually

Table 1. Results for the equilibrium lattice constant a, equilibrium volume Ω_0, the bulk modulus B and the c/a ratio of the α (hcp) titanium structure, in comparison with experimental data. Results for the ω and bcc relative phase stability (in eV/atom) tests are also included. The two theoretical values from Reference [32] are due to two different exchange-correlation potentials.

	a (Å)	B (GPa)	Ω_0 (Å^3)	c/a ratio (hcp)	$E_\omega - E_{hcp}$	E_{bcc}–E_{hcp}
Present work	2.930	112	17.26	1.585	−0.01	0.11
Published theory						
LAPW	2.866[b], 2.925[b]	127[b], 108[b]	17.29[b], 16.18[b]	1.586[b], 1.595[b]	–	–
FP-LMTO		108[c], 125[d]		1.585[c], 1.589[d]		
Experiment	2.9506[a]	110[a]	17.64[a]	1.586[a]	–	–

[a][31]; [b][32]; [c][33]; [d][34].

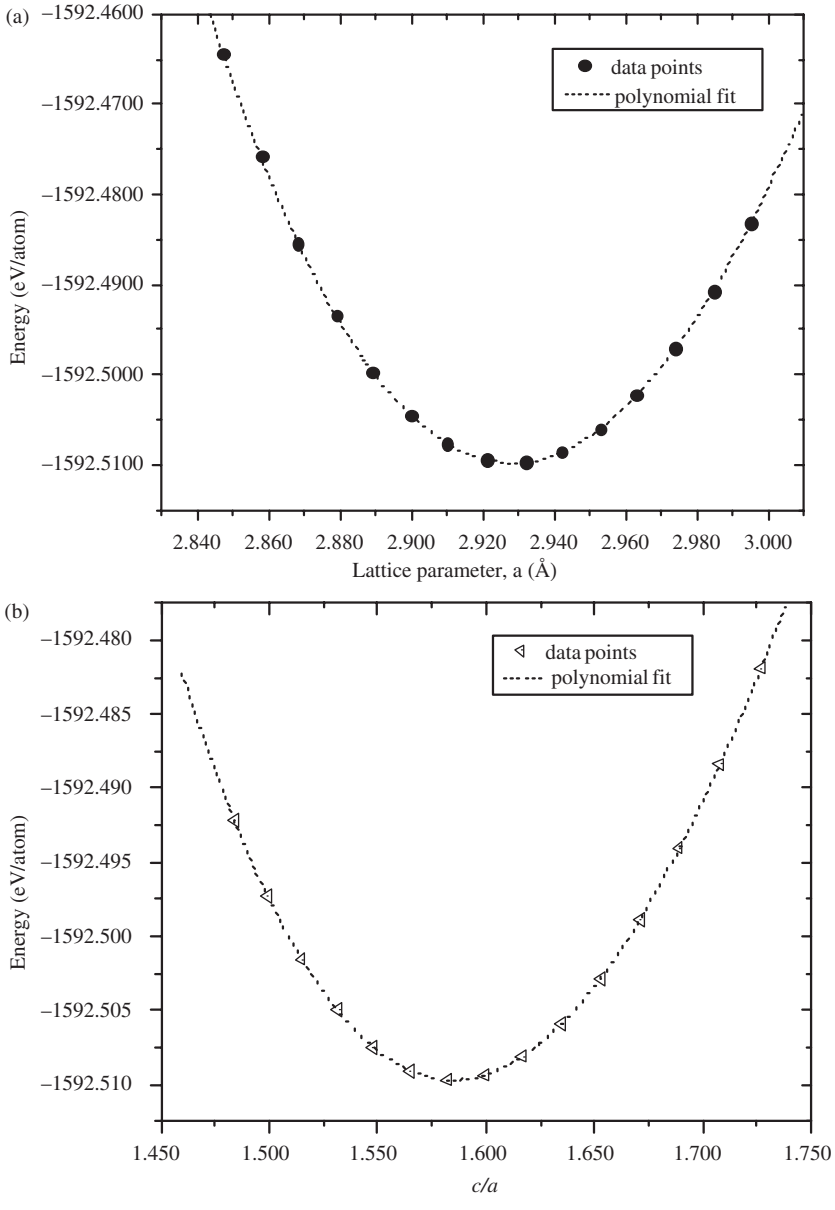

Figure 3. (a) Variation of lattice energy (eV) per atom with the lattice parameter *a*. (b) Variation in lattice energy (eV) per atom with the *c*/*a* ratio.

overestimate the equilibrium volume (Ω_0) and underestimate the bulk modulus (B). Across the transition metal (TM) series, however, and in agreement with our results, the tendency to underestimate Ω_0 in the beginning of the series (such as in Ti and V), and to overestimate Ω_0 at the end of the series (such as in Os, Ir and Pt), is a well established trend [33].

Table 2. Elastic constants (GPa) of hcp Ti, as calculated in the present work and compared with experimental values at 4 K. The experimental values are taken from [37].

	C_{11}	C_{12}	C_{13}	C_{33}	C_{44}	B_0 (GPa)
Present work (GGA)	194	69	80	175	41	114
Experiment	176	87	68	191	51	110

We summarise our theoretical elastic constants and compare with experimental results in Table 2. Overall, the agreement with experiment [38] is good in light of the expected density functional error for elastic constants of metals. The agreement is satisfactory for the bulk, B, C_{11} and C_{33} moduli. Also, using the theoretical data of Table 1, the calculated B, i.e. 110 GPa, is consistent with the 112 GPa obtained from the Murnaghan fit. However, the shear moduli C_{12} and C_{44} are underestimated, while C_{13} is overestimated. The main problem with C_{12} and C_{13} may be due to unfavourable error propagation in the evaluation of these elastic constants. The deformations [26] used to extract C_{12} and C_{13} involve a linear combination of elastic constants which are twice as large as C_{12} and C_{13}. Consequently, the relative error associated with the deformations is increased for each. Furthermore, the error in C_{12} may not be only attributed to calculation, but also to experiment, as C_{12} is known to be particularly sensitive to experimental error [39]. As regards to C_{44}, the same error margin (~20%) has been reported in previous [18,40] GGA calculations in α-Zr.

4. Results and discussions

4.1. *Vacancies*

The calculated mono and divacancy formation energies from our first principles calculations are shown in Table 3. While supercells of size $N = 16$, 32 are too small to cancel the effect of vacancy–vacancy interactions, the value of E^f_{1v} for the $N = 48$ supercell is higher than that of the largest employed cell, $N = 96$, by only 0.05 eV. The difference between the E^f_{1v} value for $N = 72$ and $N = 96$ is about 0.01 eV. Convergence with respect to supercell size can, thus, be said to have been fully achieved with $N = 72$; however, the $N = 48$ and $N = 64$ supercells yield formation energies close to the converged value as well. Our calculated value for the monovacancy formation energy in hcp titanium is thus 1.97 eV. This value is not in good agreement with either the experimental value reported by Shestopal [41], which is 1.55 eV, or the more recent positron annihilation measurements [42], which give 1.27 eV. With regards to previous theoretical studies, we have compared our result with *ab initio* data obtained using the full-potential linearised muffin-tin orbital (FP-LMTO) method [34], the full potential Green's function method [6], and the GGA calculation of Trinkle et al. [43]. They reported 2.14, 2.13 and 2.03 eV, respectively. However, our calculated value of E^f_{1v} in hcp Ti is consistent with the following correlation stated for metals [34], i.e. $H_f\,(\mathrm{eV}) = 10^{-3}\,T_m\,(\mathrm{K})$, where T_m is the melting temperature. With $T_m = 1948$ K for titanium [44], $E^f_{1v} \approx 1.95$ eV. Surface energy corrections to GGA vacancy formation energy values in metals

Table 3. Monovacancy formation energy E^f_{1v} and formation volume Ω^f_{1v} for different supercell sizes. Available experimental results are also shown for comparison. There is no reliable experimental result for monovacancy formation volume.

	Supercell sizes, N (present work)							
	16	36	48	64	72	96	Published theory	Experiment
E^f_{1v}(eV)	2.070	1.957	1.920	1.920	1.980	1.970	2.13[a] 2.14[b] 2.03[c]	1.27[d] 1.55[e]
Ω^f_{1v}	$0.54\Omega_0$	$0.67\Omega_0$	$0.64\Omega_0$	$0.64\Omega_0$	$0.64\Omega_0$	$0.64\Omega_0$	$0.60\Omega_0$[b]	

[a][6]; [b][34]; [c][42]; [d][40]; [e][41].

have been shown to reduce the discrepancy with experiments by increasing the theoretical value [45]. Thus, applying such corrections to our vacancy formation energy value for titanium, i.e. 1.97 eV, may not to lead to better agreement with experiments. This suggests that the calculations still need to be further improved. The formation volume, Ω^f_{nv} calculated according to the procedure described earlier, and using supercells containing $N = 16, 36, 48, 72$ atomic sites are also reported in Table 3. The calculated value can be said to have converged for $N = 48$, since the difference with the value obtained with $N = 36$ is negligible. Thus, $\Omega^f_{1v} = 0.64\,\Omega_0$ is our calculated monovacancy formation volume. This is in good agreement with the value calculated in [34], i.e. $\Omega^f_{1v} = 0.60\,\Omega_0$. It should be noted that there is no reliable experimental value for the titanium monovacancy formation volume.

Supercells containing 64 atomic sites have been used to investigate the D_{v1} and D_{v2}, while $N = 72$ was used for the D_{v3} configuration. The divacancy binding energies for the D_{v1} and D_{v2} configurations were calculated using the vacancy formation energy obtained for the $N = 64$ supercell size, i.e. 1.92 eV, while the binding energy for the D_{v3} configuration was calculated using the formation energy for the $N = 72$ supercell, that is, 1.98 eV. From Table 4, we note that the binding energies for the D_{v1} and D_{v2} divacancy configurations are both positive, i.e. $E^B_{2v} = 0.10$ eV and 0.12 eV, respectively. This suggests that each of the two divacancy configurations is stable compared to two isolated single vacancies. In contrast, the D_{v3} divacancy configuration has a strong negative binding energy of -0.32 eV, implying strong repulsion between the vacancies, and is thus likely to be a metastable configuration.

With regard to the structural relaxation of the atoms around a monovacancy, atoms surrounding the vacancy in the basal plane undergo inward relaxation of about $5.46 \times 10^{-3}\,a$, where $a = 2.930$ Å is the calculated basal lattice constant of titanium. The nearest neighbour atoms, i.e. those above and below the basal plane, undergo a relaxation of $7.96 \times 10^{-3}\,a$ towards the vacancy. It should be noted that structural relaxations in the hcp structure are generally believed to be small [34]. Furthermore, in hexagonal metals with a c/a ratio less than the ideal value of 1.633, such as titanium, the three atoms above and below the basal plane are at slightly

Table 4. Divacancy formation energy (E^f_{2v}), binding energy (E^B_{2v}) and formation volume Ω^f_{2v}. For the D_{v1} and D_{v2} configurations, $N=64$ supercell was used with the vacancy formation energy, $E^f_{1v}=1.92$ eV, while $N=72$ supercell was used for the D_{v3} configuration with $E^f_{1v}=1.98$ eV.

Divacancy	E^f_{2v}(eV)	E^B_{2v}(eV)	Ω^f_{2v}
In-plane (D_{v1})	3.74	0.10	$1.248\Omega_0$
Out of plane (D_{v2})	3.72	0.12	$1.314\Omega_0$
Basal to basal (D_{v3})	4.28	−0.32	$1.346\Omega_0$

Table 5. Formation energies and relaxation volumes for various interstitial configurations in hcp titanium. The asterisk (*) in the table indicates that a supercell of size $N=97$ was required to reach acceptable convergence for the BS interstitial configuration. The T configuration decays to S, while both BT and BC decay to the BO configuration.

Configurations	O	C	S	BO	BS
Formation energy (eV)					
$N=37$					
Relaxed	2.22	2.50	2.51	2.32	2.62
Unrelaxed	2.26	2.50	2.76	2.36	2.92
$N=65$					
Relaxed	2.13	2.53	2.48	2.25	2.39 (2.45*)
Unrelaxed	2.28	2.68	2.62	2.39	2.57
Relaxation volume (Ω)					
$N=37$	1.17	1.30	1.22	1.15	1.19
$N=65$	1.35	1.26	1.30	1.13	1.25

closer distances than those in the basal plane [46]. The observed displacement pattern of the atoms is, therefore, expected.

4.2. *Self-interstitials*

The interstitial formation energies for both constant volume and fully relaxed configurations are reported in Table 5. Only stable interstitial configurations, as well as the relaxation volumes for the fully relaxed configurations are shown. The effect of full relaxation is not very significant. As expected, the formation energies of fully relaxed configurations are less than that of constant volume calculations. However, the maximum energy difference between the configurations is only about 0.3 and 0.15 eV for $N=37$ and $N=65$, respectively. Also, relaxation does not affect the relative stability of the configurations in the two supercell sizes. In addition, in all the interstitial configurations, the relaxation volumes are only slightly greater than one atomic volume, in agreement with similar empirical studies in hcp metals [47], and specifically, in hcp zirconium [12]. Comparison between $N=37$ and $N=65$ atom

supercell results for the fully relaxed configurations shows that the interstitial formation energies do not change significantly between these two supercell sizes for all the studied configurations, except BS. The differences are 0.03 eV for S and C configurations, and less than 0.1 eV for the O configuration. In the case of the BS configuration, it was observed that the difference in the calculated formation energy between the two supercell sizes is 0.23 eV. Hence, we have used a supercell of size $N = 96$ to ascertain the convergence of the formation energy to 2.45 eV. With the exception of the BS configuration, therefore, the formation energies for all the interstitial configurations can be said to have converged for a supercell of 64 atoms. The O and BO configurations have the lowest formation energies consistent with results obtained in GGA calculations in hcp Zr [12], while the C configuration has the largest formation energy. The overall spread in energies is not large, ranging between 2.13 and 2.53 eV for the fully relaxed 64-atom supercell. In addition, compared to similar studies on body-centred cubic (bcc) transition metals (TM) [48], the interstitial formation energies are low. However, a close look at those calculated for transition metal groups 5B and 6B in [48] shows a substantial decrease in formation energy across the period, and an increase, down the group. For example, from Cr to V, Mo to Nb, and W to Ta, the formation energies are substantially reduced for all the interstitial configurations reported. A similar trend is observed for $W \rightarrow Mo \rightarrow Cr$ and $Ta \rightarrow Nb \rightarrow V$. If the energy values reported in [18] for octahedral (2.84 eV), crowdion (3.08 eV) and dumbbell (3.01 eV) interstitial configurations in zirconium are taken into consideration, there is indeed a substantial decrease in formation energy from Nb to Zr. We may, therefore, expect a similar pattern of results, from V to Ti, or even from Zr to Ti.

Based on the calculated formation energies, two configurations (O and BO) are probably the most stable configurations in hexagonal phase titanium. The energy differences between them are quite small, i.e. 0.12 eV. The small energy differences are also suggestive of possible co-existence of these configurations. Configurations S, C and BS appear to be less stable. Making a firm prediction of interstitial stability is generally tricky, especially when relatively small supercell sizes, as used in this work, are considered, since interstitials induce long-range stress fields. To make more quantitative predictions, therefore, larger supercell may be needed to study the effect of the elastic interaction of an interstitial with its periodically repeated images. Nevertheless, a comparison of our results with similar *ab initio* studies conducted using larger supercell sizes, in hexagonal closed packed Zr, shows good agreement in term of the relative stability of the interstitial configurations. Willlaime [18] concluded that, in hcp Zr, the most stable interstitial configurations are likely to be O, S, BC and BO, while the C configuration appears to be less stable, in good agreement with our observation for hcp Ti. Domain et al. [12] observed that five configurations, i.e. O, BO, BC, S and C, are more stable than the BT configuration in hcp Zr. The energy difference between these five configurations are, however, small, suggesting their possible co-existence under irradiation. In addition, their relative concentration may also depend on differences in vibrational entropy [17] or in electronic formation entropy [9], resulting from temperature change.

The symmetry of the hcp lattice is such that the defects and the surrounding atoms can undergo large relaxation from the initial configuration. The three atoms forming the equilateral triangle around the BO are pushed equally outward

by about 0.6 Å. The two interstitial atoms forming the BS configuration also appear to be pushed apart, and are slightly displaced from the line passing through their sites. The atoms forming the cage around the O interstitial are equally displaced outward: the strain field is symmetric. The O atom itself indeed appears to have maintained its initial input symmetry. Furthermore, both BT and BC configurations decay to BO, and the T configuration decays to S.

Extensive reviews of theoretical models of intrinsic point defects in hexagonal closed packed metals can be found in the article by Bacon [49]. In this review, it was observed that all pair potentials that model an equilibrium hcp crystal result in c/a value equal, or very close to the ideal value of 1.633. All the defect properties modelled by these potentials are, therefore, not fully reliable, but rather serve as a possible guide to what may actually occur. Many-body potentials have been developed rapidly in the last decade, though their applications in defect studies of hcp metals are not as extensive as for the cubic systems. These potentials normally contain many-body terms, which depend on the distance between the atoms, and many-body terms, which depend on the local atomic density when an atom is embedded in the medium created by its neighbours. In addition, the potentials are usually fitted to several physical parameters, such as the c/a ratio and the elastic constants of the materials, but not to any data arising from interatomic interactions at distances less than the normal equilibrium lattice spacing, such as those encountered for interstitials. This leads to formation energies which are too large. In addition, the many-body terms are isotropic and neglect directionality in the bonding, which may be important for transition metals. Therefore, these potentials offer only a simplified description of the real situation [50]. Ackland [51], using such potentials in titanium, has predicted that only SIAs within the basal plane, that is BS, BC and BO, are stable. Fernandez et al. [17], using the embedded atom potentials, also predicted BS and BC to be the most stable. Mikhin et al. [52] suggest BO as the most stable configuration, while Bacon [49] concluded that both basal and non-basal SIAs are likely to be stable in metals with $c/a \leq 1.633$. In most hcp metals studied by Igarashi et al. [53], using many-body potentials, the energetically most favourable interstitial configuration is the crowdion associated with the site C. However, the interstitial at the octahedral site O possesses, in these cases, only a marginally higher energy. Therefore, both O and C may likely co-exist as common interstitial configuration. Oh and Jonson [54], employing EAM potentials for Mg, Ti and Zr, showed the site C as energetically most favourable and the site O having a slightly higher energy. They also showed that sites S, T, BO and BC show higher energies or are unstable. Pasianot et al. [55] also predicted BC and BO to be the most stable configurations for Zr and Ti. Willaime et al. [56], using many body interatomic potential for their calculations, predict that, in hcp Zr, both S and T configurations are unstable, and both decay to C. In addition, their calculations also suggest that BC and BT are also unstable and decay to BO, in agreement with our results. From the experimental side, Huang's X-ray diffuse scattering measurement on electron irradiated single crystal hcp zirconium, at liquid helium temperature, suggests O, S and T as the most stable configurations [12]. Also, internal friction measurements [57,58] on neutron-irradiated Ti and Zr polycrystalline wires at 77 K show peaks that have been attributed to the C configuration [55]. This study concludes, from an *ab initio* energetics point of view, that the O and BO interstitial configurations are

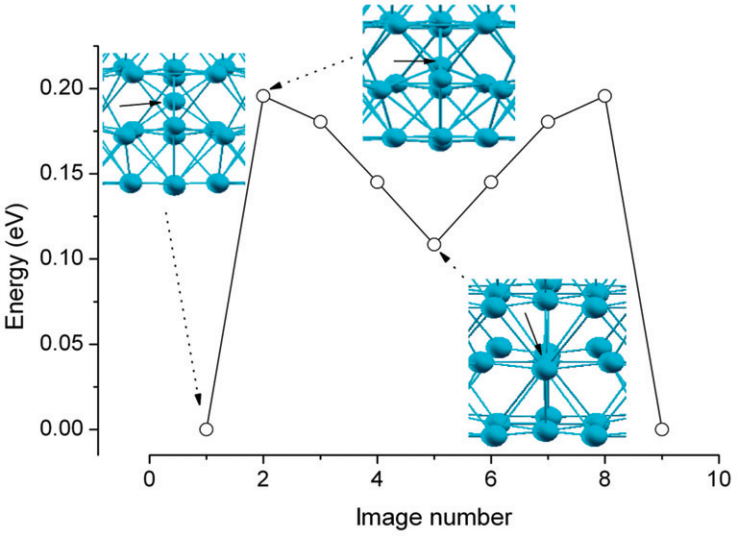

Figure 4. Minimum-energy path (MEP) for self-interstititial O–BO–B migration in a 64 atom titanium supercell. Shown on top of the MEP are the relaxed local structures of initial, transition, and intermediate states. The structure of the final state coincides with the initial one and is therefore not shown. Thick black arrows on the structures point to the positions of self-interstitial atoms.

more likely stable interstitial configurations in hexagonal closed packed titanium. The small energy differences between these configurations make their possible co-existence an equally likely possibility. In addition, we conclude that the T, BC and BT are metastable: T decays to S, while both BC and BT decay to the BO configuration.

The minimum energy path (MEP), calculated using the nudged elastic method, for the migration of a self-interstitial titanium atom from an octahedral position to the nearest octahedral position, along the *c* direction, is shown in Figure 4. Once the NEB has shown that the MEP is such that the self-interstitial atom, starting at the O site, passes through the BO configuration at halfway, we used three intermediate images between these two configurations to locate the saddle point and to determine the migration energy barrier. The other half of the MEP path, that is, from BO to O (i.e. image 6–9), has been obtained by symmetry considerations. The BO configuration appears to be a local minimum. The local structures of the initial state (image 1), the transition state (image 2) and the local minimum (image 5) are also shown. The local minimum is about 0.11 eV higher in energy than the initial state (image 1). The three nearest neighbour atoms forming an equilateral triangle around the interstitial atom in image 5 are radially equally displaced. Images 6, 7, 8 and 9 are mirrors of images 4, 3, 2, 1, respectively. In addition, one can also see that the self-interstitial atom moves from O to the BO position via a configuration that lies inbetween them. This configuration corresponds to image 2 in Figure 4, and it appears to represent the first saddle point for the interstitial atom migration. As earlier explained, the second saddle point corresponding to image 2 should be the image 8. The NEB calculated migration energy barrier for diffusion is low,

i.e. approximately 0.20 eV. Finally, it should be emphasised that a better description of Ti self-interstitial atom migration may be obtained by increasing the number of images used in the NEB calculations. However, increasing the number of images is not likely to significantly change the quantitative result on the migration energy barrier, within the accuracy of calculations.

5. Conclusion

We have performed state-of-the-art *ab initio* simulations of intrinsic point defect structures (vacancies and interstitials) in hcp titanium. The calculated monovacancy formation energy is in good agreement with other computational studies. However, agreement with the reported experimental data is not very good. Surface energy corrections to the calculated monovacancy formation energy value are unlikely to reduce the discrepancy with the experiment. This may indicate that the calculations need to be further improved. The in-plane and off-plane divacancy configurations have also been shown to be equally stable. The O and BO configurations have been predicted to be the most likely stable interstitial configurations in hcp titanium. The energy difference between the two configurations is small, suggesting their possible co-existence. The migration barrier for the diffusion of self-interstitial titanium atoms from an octahedral position to the nearest octahedral site, along the *c*-direction, is calculated to be approximately 0.20 eV.

Acknowledgements

This work was supported by the South African National Research Foundation (NRF). One of the authors, ATR, wishes to acknowledge the Mori Foundation for a scholarship award through the Abdus Salam ICTP for his visit to the institute. We have also benefited immensely from our discussions with Roger Rousseau. Most of the computations were done using the facilities at CINECA, the Italian supercomputing centre.

References

[1] P. Söderlind, L.H. Yang and J.A. Moriarty, Phys. Rev. B 61 (2000) p.2579.
[2] S. Han, L.A. Zepeda-Ruiz, G.J. Ackland, R. Car and D.J. Srolovitz, J. Appl. Phys. 93 (2003) p.3328.
[3] M.I. Mendelev, S. Han, W.-J. Son, G.J. Ackland and D.J. Srolovitz, Phys. Rev. B 76 (2007) p.214105.
[4] R. Pawellek, M. Fahnle, C. Elsässer, K.M. Ho and C.T Chan, J. Phy. Condens Mater. 3 (1991) p.2451.
[5] W. Frank, U. Breier, C. Elsässer and M. Fähnle, Phys. Rev. B 48 (1993) p.7676.
[6] B. Drittler, M. Weinert, R. Zeller and P.H. Dederichs, Solid State Commun. 79 (1991) p.31.
[7] L.A Zepeda-Ruiz, J. Rottler, S. Han, G.J. Ackland, R. Car and D.J. Srolovitz, Phys. Rev. B 70 (2004) p.060102.
[8] V. Gavini, K. Bhattacharya and M. Oritz, Phys. Rev. B 76 (2007) p.180101.
[9] W. Frank, U. Breir, C. Elsasser and M. Fähnle, Phys. Rev. Lett. 77 (1996) p.518.

[10] S. Han, L.A. Zepeda-Ruiz, G.J. Ackland, R. Car and D.J. Srolovitz, Phys. Rev. B 66 (2002) p.220101.
[11] K. Nordlund, J. Keinonen, M. Ghaly and R.S. Averback, Nature 398 (1999) p.49.
[12] C. Domain and A. Legris, Phil. Mag. 85 (2005) p.569.
[13] D.T. Britton and M. Härting, Adv. Eng. Mater. 4 (2002) p.629.
[14] M. Harting, S. Nsengiyumva, A.T. Raji, G. Dollinger, P. Sperr, S.R. Naidoo, T.E. Derry, C.M. Comrie and D.T. Britton, Surf. Coat. Tech. 201 (2007) p.8237.
[15] D. Sheppard, R. Terrell and G. Henkelman, J. Chem. Phys. 128 (2008) p.134106.
[16] C.N. Tome, A.M. Monti and E.J. Savino, Phys. Status Solidi (b) 92 (1970) p.323.
[17] J.R Fernandez, A.M. Monti and R.C. Pasianot, J. Nucl. Mater. 229 (1996) p.1.
[18] F. Willaime, J. Nucl. Mater. 323 (2003) p.205.
[19] R.A. Johnson and J.R. Beeler, *Point defects in Titanim*, in *Interatomic Potentials and Crystalline Defects*, J.K. Lee ed., AIME, New York, 1981, p.165.
[20] S. Baroni, A. Dal Corso, S. De Gironcoli and P. Giannozzi, QUANTUM-ESPRESSO; software available at http://www.pwscf.org, and http://quantum-espresso.org
[21] D. Vanderbilt, Phys. Rev. B 41 (1990) p.7892.
[22] J.P. Perdew and Y. Wang, Phys. Rev. B 45 (1992) p.13244.
[23] H.J. Monkhorst and J.D. Pack, Phys. Rev. B 13 (1976) p.5188.
[24] M. Methfessel and A.T. Paxton, Phys. Rev. B 40 (1989) p.3616.
[25] G. Henkelman, B.P. Uberuaga and H. Jónsson, J. Chem. Phys. 113 (2000) p.9901.
[26] L. Fast, J.M. Wills, B. Johansson and O. Eriksson, Phys. Rev. B 51 (1995) p.17431.
[27] F.D. Murnaghan, Proc. Natl. Acad. Sci. USA 30 (1944) p.244.
[28] D.A. Andersson and S.I. Simak, Phys. Rev. B 70 (2004) p.115108.
[29] H.K. Sahu, S. Srinivasan and K. Krishan, Radiat. Effect. Lett. 50 (1980) p.73.
[30] A. Chroneos, R.W. Grimes, B.P. Uberuaga, S. Brotzmann and H. Bracht, Appl. Phys. Lett. 91 (2007) p.192106.
[31] C.S. Barrett and T.M. Massalski, *Structure of Metals*, McGraw Hill, New York, 1966.
[32] Z.-W. Lu, D. Singh and H. Krakauer, Phys. Rev. B 36 (1987) p.7335.
[33] V. Ozoliņš and M. Körling, Phys. Rev. B 48 (1993) p.18304.
[34] O. Le Bacq, F. Willaime and A. Pasturel, Phys. Rev. B 59 (1999) p.8508.
[35] R. Ahuja, L. Dubrovinsky, N. Dubrovinskaia, J.M. Osorio, G.M. Mattesini, B. Johansson and T. Le Bihan, Phys. Rev. B 69 (2004) p.184102.
[36] Y.K. Vohra and P.T. Spencer, Phys. Rev. Lett. 86 (2001) p.3068.
[37] D.E. Trinkle, R.G. Hennig, S.G. Srinivasan, D.M. Hatch, M.D. Jones, H.T. Stokes, R.C. Albers and J.W. Wilkins, Phys. Rev. Lett. 91 (2003) p.025701.
[38] E.S. Fisher and C.J. Renken, Phys. Rev. 135 (1964) p.A482.
[39] N. Benbattouche, G.A. Saunders, E.F. Lambson and W. Honle, J. Phys. D 22 (1989) p.670.
[40] C. Domain, R. Besson and A. Legris, Acta Mater. 50 (2002) p.3513.
[41] V.O. Shestopal, Sov. Phys. Solid State 7 (1966) p.2798.
[42] E. Hashimoto, E.A. Smirnov and T. Kino, J. Phys. F Met. Phys. 14 (1984) p.L215.
[43] D.E. Trinkle, M.D. Jones, R.G. Hennig, S.P. Rudin, R.C. Albers and J.W. Wilkins, Phys. Rev. B 73 (2006) p.094123.
[44] R.M. Tennet (ed.), *Science Data Book*, Oliver and Boyd, Edinburgh, 1978.
[45] K. Carling, G. Wahnström, T.R. Mattsson, A.E. Mattsson, N. Sandberg and G. Grimvall, Phys. Rev. Lett. 85 (2000) p.3862.
[46] P.G. Partridge, Met. Rev. 118 (1967) p.169.
[47] R.A. Johnson, Phil. Mag. A 63 (1991) p.865.
[48] D. Nguyen-Manh, A.P. Horsfield and S.L. Dudarev, Phys. Rev. B. 73 (2006) p.020101.
[49] D.J. Bacon, J. Nucl. Mater. 159 (1988) p.176.
[50] D.J. Bacon, J. Nucl. Mater. 206 (1993) p.249.

[51] G.J. Ackland, Phil. Mag. A 66 (1992) p.917.
[52] A.G. Mikhin, Y.N. Osetsky and V.G. Kapinos, Phil. Mag. A 70 (1994) p.25.
[53] M. Igarashi, M. Khantha and V. Vitek, Phil. Mag. B 63 (1991) p.603.
[54] D.J. Oh and R.A. Johnson, J. Mater. Res. 3 (1988) p.471.
[55] R.C. Pasianot and A.M. Monti, J. Nucl. Mater. 264 (1999) p.198.
[56] F. Willaime and C. Massobrio, Phys. Rev. B. 43 (1991) p.11653.
[57] R. Pichon, E. Bisogni and P. Moser, Radiat. Effect. 22 (1974) p.173.
[58] R. Pichon, E. Bisogni and P. Moser, Radiat. Effect. 20 (1973) p.159.